Toxicology Letters 252 (2016) 29–41

Contents lists available at ScienceDirect

Toxicology Letters

journal homepage: www.elsevier.com/locate/toxlet

Molecular mechanisms of endocrine and metabolic disruption: An *in silico* study on antitrypanosomal natural products and some derivatives

Zhenquan Hu, Joël Wahl, Matthias Hamburger, Angelo Vedani*

Department of Pharmaceutical Sciences, University of Basel, Basel, Switzerland

HIGHLIGHTS

- Antitrypanosomal active natural products may trigger endocrine disregulation.
- Only few antitrypanosomal active natural products sustain drug–drug interactions.
- More complex toxic endpoints may be elucidated by molecular simulations.
- The *VirtualToxLab* allows identifying side effects and associated molecular mechanisms.
- The *VirtualToxLab* is freely available for academic and non-profit organizations.

GRAPHICAL ABSTRACT

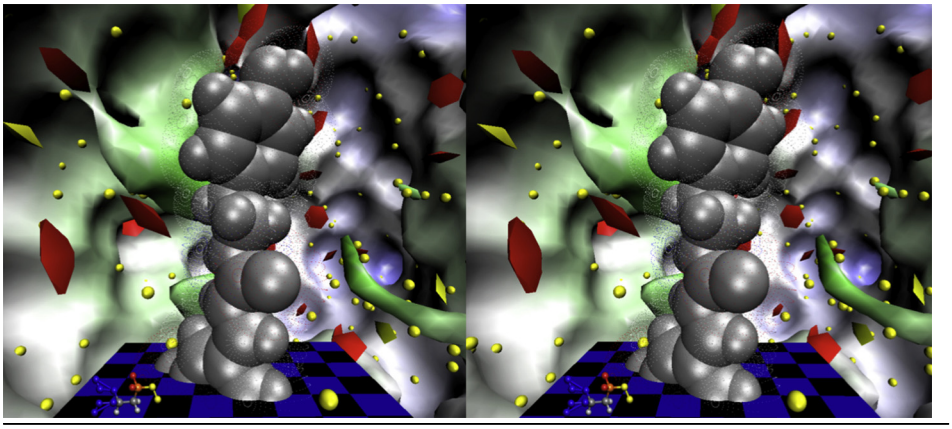

ARTICLE INFO

Article history:
Received 20 February 2016
Received in revised form 12 April 2016
Accepted 14 April 2016
Available online 16 April 2016

Dedicated to Professor Edgar F. Meyer, mentor and friend—deceased 2015.

Keywords:
VirtualToxLab
Adverse effects
In silico profiling
Molecular-dynamics simulations
Antitrypanosomal natural products

ABSTRACT

The *VirtualToxLab* is an *in silico* technology for estimating the toxic potential – endocrine and metabolic disruption, as well as aspects of carcinogenicity and cardiotoxicity – of drugs, chemicals and natural products. The technology is based on an automated protocol that simulates and quantifies the binding of small molecules towards a series of currently 16 proteins, known or suspected to trigger adverse effects. The simulations are conducted at the atomic level and explicitly allow for a mechanistic interpretation of the results (in real-time 3D/4D), thereby complying with the Setubal principles put forward in 2002 for computational approaches to toxicology. Moreover, the underlying "*ab-initio*" protocol is independent from any training data and makes the approach universal with respect to the applicability domain. The *VirtualToxLab* runs in client–server mode and is freely available to academic and non-profit organizations. As the underlying technology yields a thermodynamic estimate of the binding affinity, the associated ligand–protein complexes have been challenged by molecular-dynamics simulations to probe their kinetic stability.

Human African trypanosomiasis is a neglected tropical disease caused by two subspecies of *Trypanosoma brucei*. The control of this parasitic infection relies on a few chemotherapeutic agents, most of which were discovered decades ago and pose many challenges including adverse side effects, poor efficacy, and the occurrence of drug resistances. Natural products, on the other hand, offer a high potential for the discovery of new drug leads due to their chemical diversity. In this *in silico* study, we analyze a series of 89 natural products and derivatives displaying anti-trypanosomal activity for their potential to trigger adverse effects. Our results indicate a moderate potential for a number of those

* Corresponding author.
E-mail address: angelo.vedani@unibas.ch (A. Vedani).

http://dx.doi.org/10.1016/j.toxlet.2016.04.013

compounds to bind to nuclear receptors and thereby ease the development of endocrine disregulation. A few others would seem to inhibit enzymes of the cytochrome P450 family and, hence, sustain drug–drug interactions.

1. Introduction

In silico techniques for the prediction of toxicological endpoints are extremely attractive because they are typically fast, inexpensive and can be applied to both existing and hypothetical compounds. Concepts in computational toxicology may be classified into expert systems, QSAR (quantitative structure–activity relationships), protein modeling and ADME (adsorption, distribution, metabolism, excretion) modeling. A large body of both review and research articles exists for these technologies (see, for example, Piclin et al., 2006; Amini et al., 2007; Aronov et al., 2007; Bender et al., 2007; Custer et al., 2007; Ecker and Chiba, 2007; Ekins, 2007; Serafimova et al., 2007; Enoch et al., 2008; Kavlock et al., 2008; Merlot, 2008; Pavan and Worth, 2008; Benfenati et al., 2009; Green and Naven, 2009; Nigsch et al., 2009; Spreafico et al., 2009; Valerio, 2009; Rossato et al., 2010; Cronin and Madden, 2010; Bars et al., 2011; Vuorinen et al., 2013; Gupta et al., 2013; Roncaglioni et al., 2013; Shah and Greene, 2014; Toropov et al., 2014; Schilter et al., 2014; Singh and Gupta, 2014; Ekins, 2014; Vedani et al., 2015; Benfenati, 2016).

Developing and validating a three-dimensional model is laborious but would seem to be necessary when the molecular mechanism triggering the adverse or toxic effect occurs via a multifaceted mode of action at the molecular level. Manifestations of toxicity are frequently mediated by regulatory macromolecules such as enzymes, receptors, ion channels or DNA. These targets represent complex and flexible three-dimensional entities that attempt to optimize their interaction with a small molecule (both natural compounds and xenobiotics) by adapting their 3D conformation, a mechanism referred to as "induced fit". Protein-bound solvent molecules are frequently involved in stabilizing small-molecule ligands or, upon release to the bulk solvent contribute favorably to the binding entropy. Accounting and quantifying these effects belongs to the most challenging tasks in the computational biosciences.

The *VirtualToxLab* (cf. http://www.virtualtoxlab.org) is an *in silico* concept for estimating the toxic potential – endocrine and metabolic disruption, aspects of carcinogenicity and cardiotoxicity – of drugs, chemicals and natural products (Vedani et al., 2012, 2015). The technology is based on an automated protocol that simulates and quantifies the binding of small molecules ($50 < MW < 1500$) towards a series of currently 16 proteins, known or suspected to trigger adverse effects: 10 nuclear receptors (androgen, estrogen α, estrogen β, glucocorticoid, liver X, mineralocorticoid, peroxisome proliferator-activated receptor γ, progesterone, thyroid α, thyroid β), four members of the cytochrome P450 enzyme family (1A2, 2C9, 2D6, 3A4), a cytosolic transcription factor (aryl hydrocarbon receptor) and a potassium ion channel (hERG). The simulations are conducted at the atomic level and explicitly allow for a mechanistic interpretation of the results in real-time 3D/4D, thereby complying with the *Setubal* principles put forward in 2002 (Worth and Cronin, 2004) for computational approaches to toxicology. Moreover, the underlying "*ab-initio*" protocol is independent from any training data and makes the approach universal with respect to the applicability domain. The toxic potential of a compound – its ability to trigger adverse effects – is derived from its computed binding affinities toward these very proteins. The computationally demanding simulations are performed in client–server mode on a Linux cluster at the University of Basel. The graphical-user interface allows building and uploading molecular structures, inspecting and downloading the results and, most important, rationalizing any prediction at the atomic level by interactively analyzing the binding mode of a compound with its target protein(s) in real-time 3D/4D. Access to the *VirtualToxLab* is available free of charge for academic institutions, public hospitals, governmental agencies, regulatory bodies and non-profit organizations (cf. http://www.biograf.ch/data/projects/OpenVirtualToxLab.php).

Molecular Dynamics (MD) simulations allow for analyzing and quantifying the interaction of a small molecule bound to a protein over an – albeit moderate – time span of typically a few nanoseconds to one microsecond. This is performed by applying Newton's law of motion to each atom of the solvated ligand–protein complex exposed to the forces acting on it through its molecular environment. Those forces are governed by an appropriate force field and allowance must be given for both structural and bulk solvent (typically water). A wealth of literature exists on both theory and application of MD simulations (see, for example, Mortier et al., 2015; Zhao and Cafliesch, 2015; Kerrigan, 2013). In our context, we analyze the stability of salt bridges and hydrogen bonds, the presence or absence of distinguished lipophilic interactions as well as the role of bound solvent. For the simulation and quantification (of the structural prerequisites) of adverse or toxic effects triggered by molecular mechanisms, MD simulations would seem to be the tool of choice to confirm (or refute) the findings obtained by thermodynamic approaches (e.g. the *VirtualToxLab*).

Human African trypanosomiasis (HAT) is a neglected tropical disease caused by two subspecies of *Trypanosoma brucei* (De Olivera et al., 2015). The associated infection is life threatening and represents a risk to large parts of the populations in poor tropical countries. The control of this parasitic infection relies on a few chemotherapeutic agents, most of which were discovered decades ago and pose many challenges due to adverse side effects, long treatment cycles, poor efficacy, high costs, the occurrence of drug resistances, and limited availability (Orhan et al., 2010; Hotez et al., 2007). Therefore, the discovery of novel, safe, and effective antiprotozoal agents remains an urgent need. Natural products play a significant role in the discovery of new drug leads because of the unmatched availability of chemical diversity (Kellenberger et al., 2011). Considering the severe disadvantages of existing drugs, there is a clear and pressing need for the development of safer and more effective drugs for the treatment of HAT. Many natural products have been reported showing antitrypanosomal activity—including flavonoids, xanthones, lignans, terpenes, and alkaloids. We recently identified several classes of natural products with promising *in vitro* antitrypanosomal activity (Kellenberger et al., 2011; Hata et al., 2011; Farimani et al., 2011; Julian et al., 2011; S'lusarczyk et al., 2011; Zimmermann et al., 2014; Ayyari et al., 2014; Usuki et al., 2014). These compounds represent a diverse and challenging series of chemicals for *in silico* profiling with respect to adverse effects.

2. Methods

2.1. The VirtualToxLab

The technology underlying the *VirtualToxLab* has been recently described in detail in this journal (Vedani et al., 2015, 2012) and

shall, therefore, only be briefly summarized in this account. It is based on a client–server protocol and consists of a graphical user interface (uploading compounds, downloading and visualizing results) and the server backend (1024-node Linux cluster where the calculations are performed). The user interface features a 3D model builder for readily generating the three-dimensional structure of any small molecule of interest, an embedded 3D viewer for inspecting the compounds to be uploaded and a 3D/4D viewer for analyzing the output structures (protein–ligand complexes). In a first step, a compound's configurations (position, orientation, conformation) in aqueous solution are sampled and quantified using the *Aquarius* software (Vedani et al., 2015; Fig. 1, left). Then, a similar protocol with allowance for induced fit is employed at the protein (Fig. 1, center) using *Alignator* (template-based alignment: Smieško, 2013) and *Cheetah* (Monte-Carlo sampling, dynamic solvation, refinement: Vedani et al., 2015; Rossato et al., 2010). In a next step, the change in free energy ΔG of the small molecule when binding from the aqueous environment to the protein is estimated (*BzScore4D*: Vedani et al., 2015).

Finally, the affinities towards all 16 target proteins are weighted and compiled into a single figure: the toxic potential ranging from 0.0 (benign) to 1.0 (extreme). Based on its value (low, intermediate, high), different follow-up procedures — including MD, PP, ADMET and consensus scoring — are then performed. For details, see Vedani (2016: Fig. 15).

The technology has been extensively validated (cf. Vedani et al., 2015, 2012 and references cited therein). The predictive power of the current version and that of the 16 individual targets are available on-line (Biographics Laboratory 3R, 2016a; Vedani, 2016: Fig. 6, respectively).

2.2. Molecular-dynamics (MD) simulations

The MD simulations were carried out in consensus mode using (i) AMBER12 (Case et al., 2012) employing the AMBER FF14sb force field (Case et al., 2014), (ii) NAMD2.9 (Phillips et al., 2005) combined with the CHARMM36 force field (Best et al., 2012) and (iii) *Desmond* (Darden et al., 1993) along with *MacroModel* (Mohamadi et al., 1990) featuring the OPLS2005 force field (Banks et al., 2005). The details of the individual protocols are given in the Supplementary data (File: MolecularDynamics.pdf). The need to augment the *VirtualToxLab* calculations by MD simulations arises from the fact that the Monte-Carlo sampling technology employed in the *VirtualToxLab* (software *Cheetah*, cf. Vedani et al., 2015; Rossato et al., 2010) computes a thermodynamic value for a compound's strength to bind to a given target protein. While this is a necessary condition for binding, it is not sufficient as the ligand–protein interaction must be stable over a reasonable period of time in order to trigger an (e.g. agonistic) effect. This kinetic aspect – i.e. the time-dependent stability of a ligand–protein complex – can be assessed reasonably well through MD simulations. The time span for which a MD simulation should be conducted is debatable; in this study we used a reasonable span time of 10^{-8} s (10 ns), which allows to safely monitor the stability of key ligand–protein interactions (e.g. hydrogen bonds) as well as the response of the protein to ligand binding (induced fit).

2.3. Antitrypanosomal compounds

The 3D structures of the employed 89 natural antitrypanosomal compounds (Farimani et al., 2011; Julian et al., 2011; S'lusarczyk et al., 2011; Ayyari et al., 2014) were generated with Bio^X (Dobler, 2014) and optimized using the directional *Yeti* force field (Vedani and Huhta, 1990). As part of the *VirtualToxLab* protocol, their conformations were exhaustively sampled in aqueous solution (Vedani et al., 2015). Their chemical structures along with the SMILES codes are given in the Supplementary data (File: Compounds.pdf). The most feasible protonation state at physiological pH (7.4) is determined by the *VirtualToxLab* (Vedani et al., 2015). The conformational variability of the compounds was assessed by exhaustive conformational sampling in aqueous solution (software *MacroModel*: Mohamadi et al., 1990); details of the underlying protocols are given in (Vedani et al., 2015, 2012).

3. Results and discussion

The results with the *VirtualToxLab* were obtained with version 5.5 (September 2015). Simulation of the binding of the 89 compounds (natural products and some derivatives) to the 16 target proteins and estimating their toxic potential required a total 6189 CPU (central processing unit) hours. Individual binding affinities and the toxic potential are shown graphically in Figs. 2 and 3, summarized in Table 1 and are given in detail in the Supplementary data (File: VirtualToxLab.xlsx).

The more frequently identified target proteins of the antitrypanosomal compounds include the androgen, estrogen α, estrogen β, glucocorticoid and aryl hydrocarbon receptor. Only rarely was binding to the enzymes of the cytochromes P450 family (as inhibitors), the Liver-X and the PPARγ observed and occasional binding to the remaining targets identified. Table 1 summarizes the binding of the most interesting findings (for details, cf. Supplementary data). For all compounds with a calculated binding

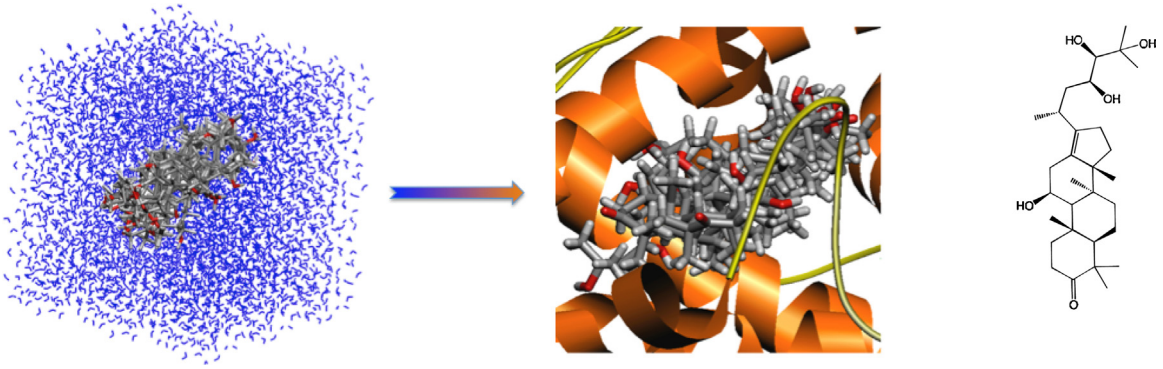

Fig. 1. 4D-Boltzmann sampling as employed in the *VirtualToxLab*. Left: a compound's (here: Alisol A, one of the investigated compounds) representations in aqueous solution. Center: sampling and quantifying the ligand's representations at the binding site of the target protein (here: the glucocorticoid receptor). For clarity, only 12 (out of 54 identified) conformations in aqueous solution and 6 (out of 24 identified) at the protein are shown. The images were generated with the Bio^X software (Dobler, 2014). Right: structure of Alisol A.

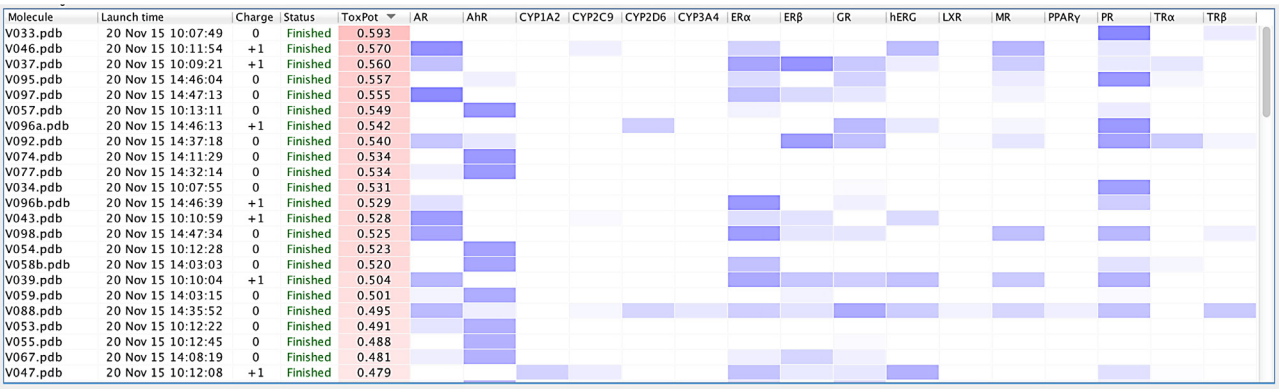

Molecule	Launch time	Charge	Status	ToxPot	AR	AhR	CYP1A2	CYP2C9	CYP2D6	CYP3A4	ERα	ERβ	GR	hERG	LXR	MR	PPARγ	PR	TRα	TRβ
V033.pdb	20 Nov 15 10:07:49	0	Finished	0.593																
V046.pdb	20 Nov 15 10:11:54	+1	Finished	0.570																
V037.pdb	20 Nov 15 10:09:21	+1	Finished	0.560																
V095.pdb	20 Nov 15 14:46:04	0	Finished	0.557																
V097.pdb	20 Nov 15 14:47:13	0	Finished	0.555																
V057.pdb	20 Nov 15 10:13:11	0	Finished	0.549																
V096a.pdb	20 Nov 15 14:46:13	+1	Finished	0.542																
V092.pdb	20 Nov 15 14:37:18	0	Finished	0.540																
V074.pdb	20 Nov 15 14:11:29	0	Finished	0.534																
V077.pdb	20 Nov 15 14:32:14	0	Finished	0.534																
V034.pdb	20 Nov 15 10:07:55	0	Finished	0.531																
V096b.pdb	20 Nov 15 14:46:39	+1	Finished	0.529																
V043.pdb	20 Nov 15 10:10:59	+1	Finished	0.528																
V098.pdb	20 Nov 15 14:47:34	0	Finished	0.525																
V054.pdb	20 Nov 15 10:12:28	0	Finished	0.523																
V058b.pdb	20 Nov 15 14:03:03	0	Finished	0.520																
V039.pdb	20 Nov 15 10:10:04	+1	Finished	0.504																
V059.pdb	20 Nov 15 14:03:15	0	Finished	0.501																
V088.pdb	20 Nov 15 14:35:52	0	Finished	0.495																
V053.pdb	20 Nov 15 10:12:22	0	Finished	0.491																
V055.pdb	20 Nov 15 10:12:45	0	Finished	0.488																
V067.pdb	20 Nov 15 14:08:19	0	Finished	0.481																
V047.pdb	20 Nov 15 10:12:08	+1	Finished	0.479																

Fig. 2. Toxic potential and binding affinities as obtained by the *VirtualToxLab* (and shown by the molecule panel in the graphical-user interface). The selection (sorted by the toxic potential) shows both values intensity-colored, i.e. the darker (toxic potential = red, affinities = blue) the more prominent the effect. Upon moving the computer mouse over an affinity field, the underlying numerical value is displayed (Vedani et al., 2015). A white field indicates "no binding", i.e. a computed binding affinity > 100 μM. (For interpretation of the references to colour in this figure legend, the reader is referred to the web version of this article.)

affinity < 100 nM, subsequent MD simulations were performed (Hu, 2015) to probe the kinetic stability of the underlying ligand–protein complex. For the more interesting thereof, MD simulations were performed in consensus mode (AMBER, CHARMM and *Desmond*, respectively). The details are given in the Supplementary data (File: MolecularDynamics.pdf). The toxic potential is computed from the individual binding affinities towards the 16 off-targets (for details, see Vedani et al., 2015; Vedani, 2016) currently included in the *VirtualToxLab*. It should be interpreted as an alert, indicating a compound's (thermodynamic) probability to trigger adverse effects. Fig. 3 (top) shows the values obtained for the 89 compounds in a pictorial way. The computed values range from 0.161 (benign) to 0.593 (potentially harmful). The distribution of this value for the natural compounds with antitrypanosomal activity indicates a moderate risk with respect of triggering adverse effects, particularly at continued exposure.

3.1. Endocrine disruption—binding to nuclear receptors

Endocrine disruption could be triggered by binding to one or several of the 10 nuclear receptors (AR, ERα, ERβ, GR, LXR, MR, PPARγ, PR, TRα, TRβ) currently tested for in the *VirtualToxLab*. Typical ligands – e.g. 17β-estradiol, bisphenol A or diethylstilbestrol – feature a lipophilic core augmented by polar ends. Nonetheless, compounds with only one polar end (e.g. substituted phenols or phtalates) are also known to bind to these entities—albeit with a smaller affinity. Among the investigated 89 antitrypanosomal compounds, 22 show a favorable interaction with one of the nuclear receptors, i.e. leading to a computed binding affinity < 100 nM (cf. Fig. 3: bottom). However, not all of these ligand–protein complexes are kinetically stable when probed by means of MD simulations (cf. below). Concerning the computed binding affinity, the interaction of **97** with the androgen receptor (Table 1 and Fig. 4) is the most noticeable. According to our simulations, the paprazine derivative engages in strong interactions with two key amino-acid residues of the receptor (Asn705 and Thr877). However, it cannot reach out (bind) to Arg752, which would be necessary for triggering an agonistic effect. Instead, it engages in a hydrogen bond with the backbone amide-H atom of Met787. Therefore, **97** might act as an antagonist (antiandrogen), which is not desirable either. The computed binding affinity is 8.4 nM, which underlines the strength of the interaction. Fig. 4 shows the thermodynamic binding mode – i.e. the energetically most favorable pose – of **97** (left) and its kinetic stability during a 10 ns MD simulation. The interactions with Asn705 and Thr877 remain stable throughout the entire simulation while the desired one with Arg752 is never truly established.[1] The total energy (of the simulation employing the main pose; blue curve) shows only small fluctuations compared with the initial state (corresponding to the thermodynamically most favorable binding mode as identified by the *VirtualToxLab*). Other compounds and targets include **98** binding to the estrogen receptor α and the mineralocorticoid receptor, **88** to the glucocorticoid receptor and **33** to the progesterone receptor (Fig. 5). Concerning **98**, it should be noted that it binds to both entities in a *cis* configuration, while the energetically more favorable mode is *trans*. A *cis* → *trans* interconversion *in situ* might be feasible but is not very probable. The binding of **33** to the progesterone receptor would seem to be of interest as the molecule is stabilized by two hydrogen bonds with Thr894 and Arg766, respectively. Compound **88** at the glucocorticoid receptor is stabilized by three hydrogen bonds with Gln670 and Arg611 and Asn564, respectively.

3.2. Cardiotoxicity—binding to the hERG ion channel

Of great interest would be to know if natural antitrypanosomal compounds might inhibit the hERG ion channel and thereby triggering cardiotoxic (arrhythmic) effects. Some of the investigated compounds would, indeed, seem to have a potential for binding to hERG—for example **47** for which an appreciable affinity of 119 nM is calculated. Fig. 6 shows the details of its proposed binding to hERG. The ammonium group ($pK_{a,calc}$ = 9.45, hence, protonated at physiological pH) engages in two hydrogen bonds with Ser61 and Ser167, respectively. The lactone carbonyl O atom forms a hydrogen bond with Tyr295 and the hydrophobic portions of the molecule are embedded in lipophilic parts of the binding pocket. As for the hERG ion channel no experimental (X-ray or NMR) 3D structure is currently available, a homology model for this protein is used instead (cf. Vedani, 2016: Table 2). Therefore, any conclusion drawn therefrom should be interpreted with care.

[1] Among the 12 identified poses, only one finds the phenolic hydroxyl O atom in the vicinity of Arg752—however, at an O···H distance of 4.8 Å, far too distant for a substantial stabilization. Consequently, that pose is computed to contribute a mere 2.8×10^{-5} to the Boltzmann ensemble. Nonetheless, we run a MD simulation starting from that very pose, testing whether the equilibration protocol might find a stronger interaction with Arg752—without success, though: a strong interaction of the hydroxyl O atom of **97** with Arg752 is only present for less than 4% of the time. At that time, the two other hydrogen bonds are significantly weakened. Throughout the entire simulation, the total protein–ligand interaction energy remains 10% weaker than that for the main pose.

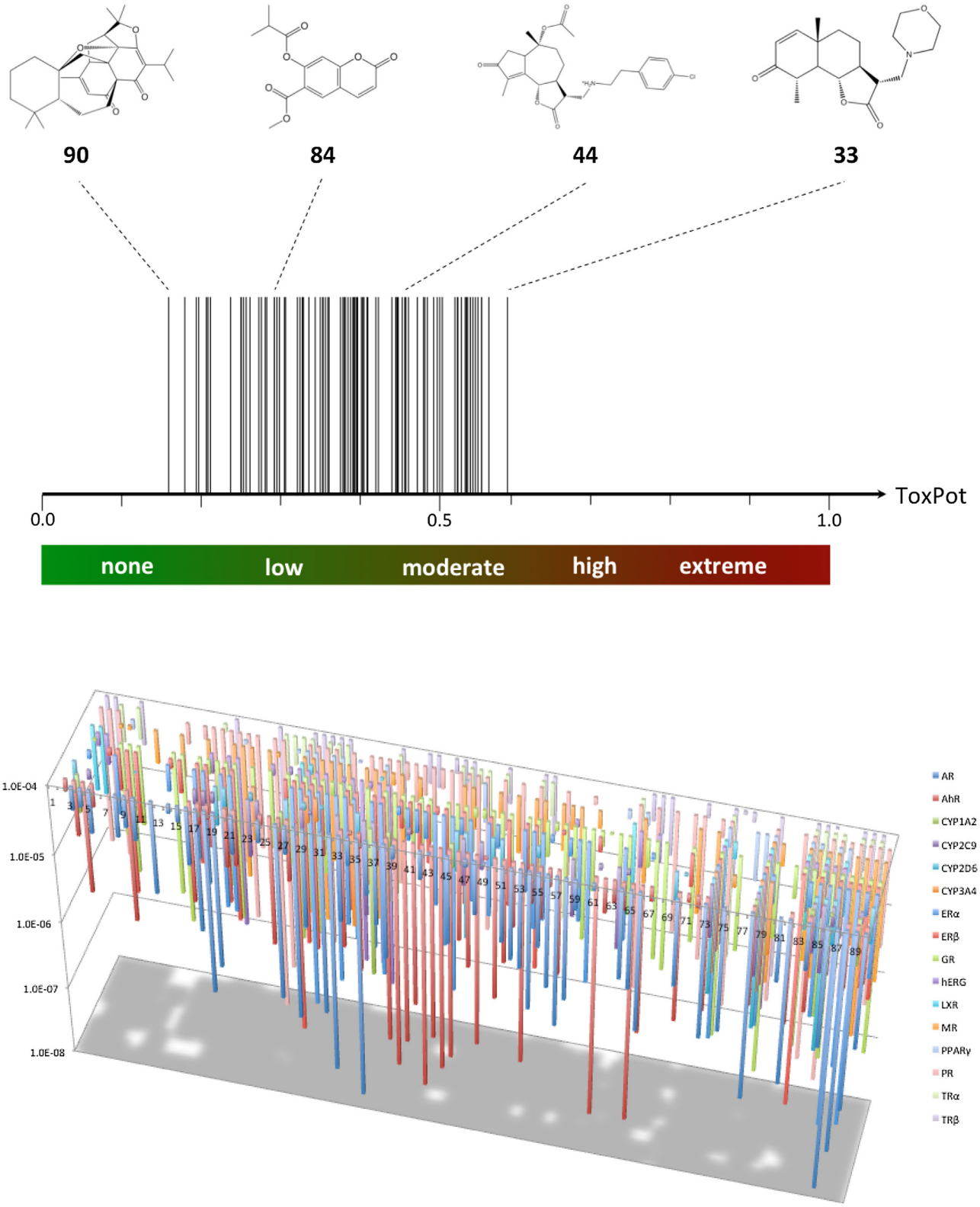

Fig. 3. Top: bandwidth of the toxic potential of the 89 antitrypanosomal compounds. Bottom: distribution of individual binding affinities over the 16 target proteins as obtained by the *VirtualToxLab*. For clarity, only affinities $< 100\ \mu M$ are depicted. The numbers on the horizontal axis correspond to the compound IDs. White spots on the floor indicate that the compound(s) display(s) no activity towards the target(s). The 3D plot and the underlying data are available in the Supplementary data in original Excel formatting.

Table 1
Four selected compounds and their suspected protein targets as identified by the *VirtualToxLab*.

ID	Structure	Main target[a] Affinity[b] Toxic potential[c]	Ligand–protein interactions (*VirtualToxLab*): Thermodynamic binding mode, i.e. energetically most favorable pose	10 ns MD simulations[d] (AMBER, CHARMM): Kinetic binding mode
33	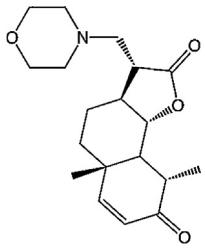	Progesterone receptor: 10.1 nM 0.593	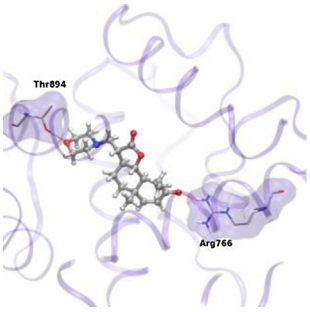	Not supportive: Hydrogen bonds with Thr894 and Arg766 are only present during 1% and 2% of the simulation time, respectively (see also Fig. 5)
37	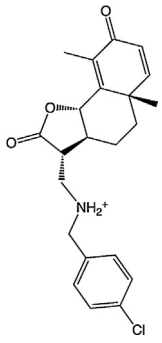	Estrogen receptor β: 20.4 nM 0.560	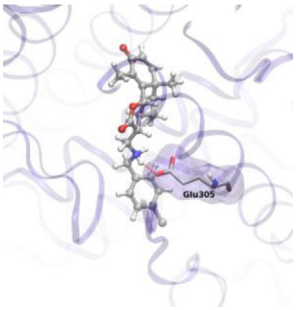	Partially supportive: Salt bridge (with the ammonium H atoms) with Glu305 is present during 92% and 17% of the simulation time, respectively. The nearby Arg346 forms a salt bridge with Glu305 (as observed in the native state) for less than 5% of the time only
54	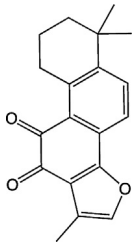	Aryl hydrocarbon receptor: 46.0 nM 0.523	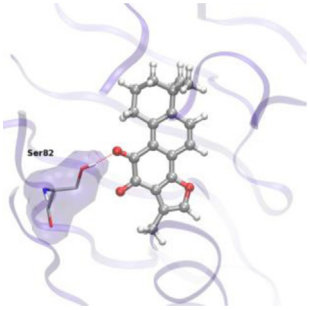	Partially supportive: The hydrogen bond with Ser82 is present during 54% of the simulation time (cf. Fig. 7)
97	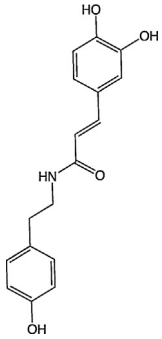	Androgen receptor: 12.7 nM 0.555	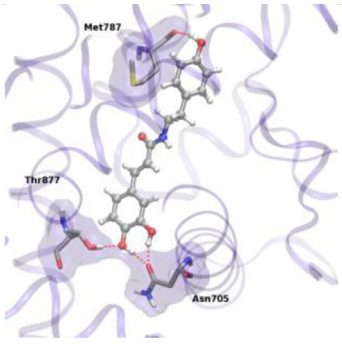	Fully supportive: Hydrogen bonds with Asn705 and Thr877/ Ser753 are present during 96% and 66% of the simulation time, respectively (cf. Fig. 4)

[a] Of the 16 tested proteins: AhR, AR, ERαβ, GR, hERG, LXR, MR, PPARγ, PR, TRαβ, 1A2, 2C9, 2D6, 3A4.
[b] Calculated by 4D Boltzmann scoring (Vedani et al., 2015; see also Fig. 12).
[c] Expected effects: TP < 0.3: no, 0.3 < TP < 0.5: weak, 0.5 < TP < 0.6: moderate, 0.6 < TP < 0.7: strong, TP > 0.7 extreme.
[d] MD is supportive, if the stabilizing hydrogen-bond interaction(s) are present throughout the entire simulation.

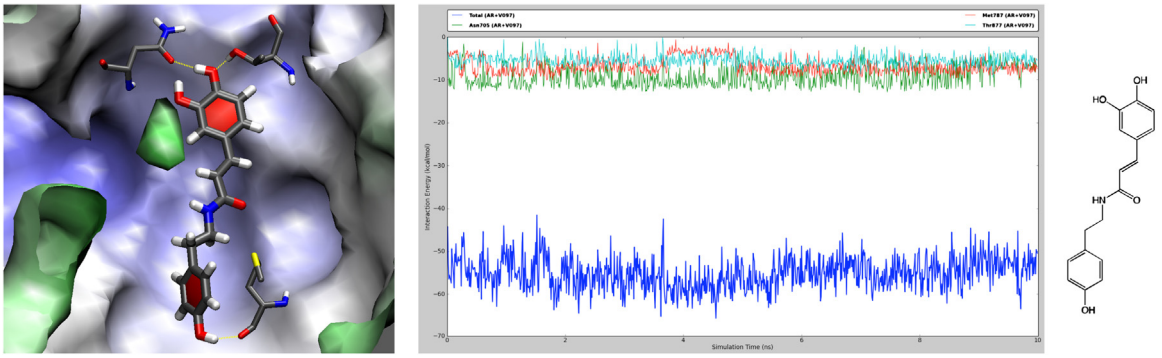

Fig. 4. Left: binding of **97** to the androgen receptor. The ligand and key amino-acid residues are shown in licorice, the protein is depicted by its inner surface (colored by z-depth). Hydrogen bonds are indicated as yellow dashed lines. The image was generated employing the VMD software (Humphrey et al., 1996). Center: 10.0 ns MD simulation indicating the stable character of the ligand–protein interactions throughout the entire simulation. Right: structure of **97**. (For interpretation of the references to colour in this figure legend, the reader is referred to the web version of this article.)

The MD simulation suggests that three serine moieties (Ser61, Ser164, Ser267) share hydrogen bonds with the ammonium group, while the *VirtualToxLab* (Monte-Carlo sampling) sticks with Ser61 and Ser164 at the lowest-energy pose. In the *VirtualToxLab* (4D representation), the serine triple is also observed, of course only in pairs at the time. This represents an agreement of the *VirtualToxLab* and the MD simulation and – in this case – of thermodynamic and kinetic approaches.

3.3. Carcinogenicity—binding to the aryl hydrocarbon receptor

A few compounds of the series might bind to the Aryl hydrocarbon receptor and, thereby, trigger mechanisms eventually leading to carcinogenic effects. An example is tanshinone, which is computed to bind with an affinity of 46 nM to this target. This is shown in Fig. 7: the aromatic and aliphatic portions of the molecule are accommodated by lipophilic amino-acid residues of the

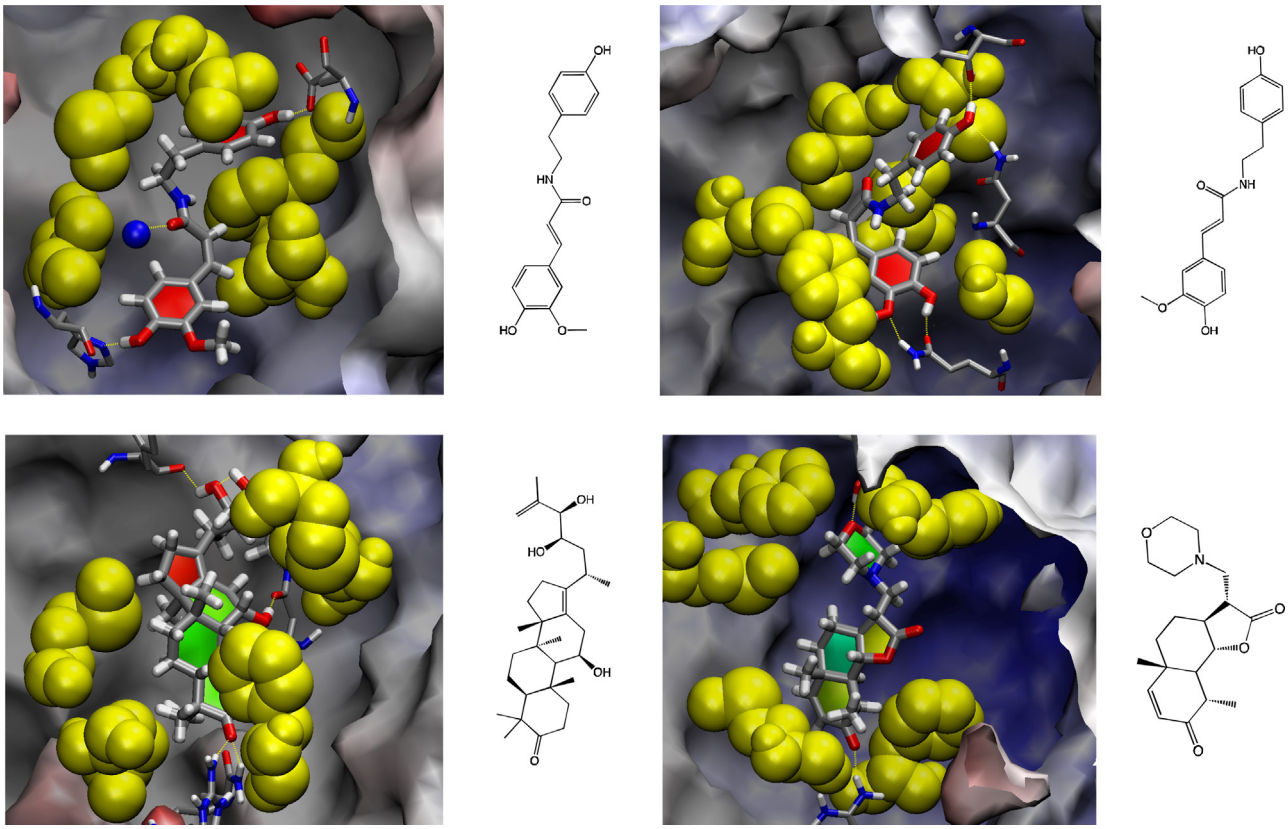

Fig. 5. Top panel: binding of **98** to the estrogen receptor α (left) and to the mineralocorticoid receptor (right). Bottom panel: binding of **88** to the glucocorticoid receptor (left) and **33** to the progesterone receptor (right). The ligand and a key amino-acid residue are shown in licorice, hydrophobic residues lining the binding pocket as yellow space-filling spheres, the protein is depicted by its inner surface (colored by z-depth) and structural water molecules by blue spheres. Hydrogen bonds are indicated as yellow dashed lines. The image was generated employing the VMD software (Humphrey et al., 1996). Right of the color plates: respective structures. (For interpretation of the references to colour in this figure legend, the reader is referred to the web version of this article.)

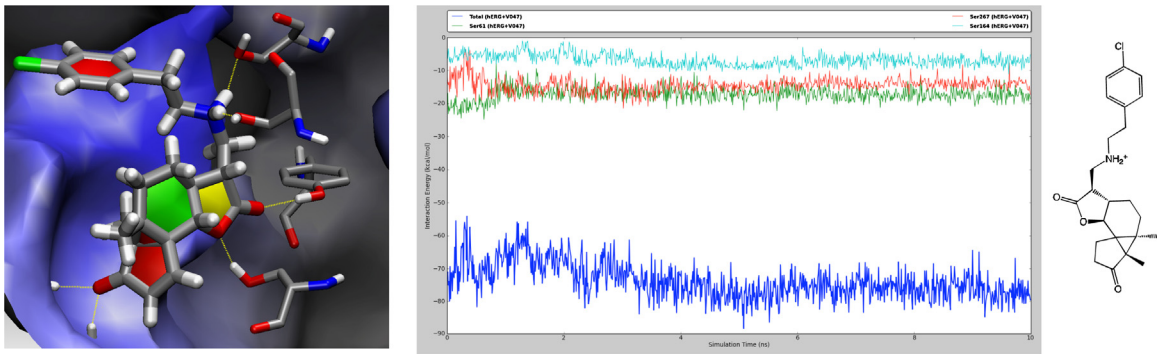

Fig. 6. Left: binding of **47** to the hERG ion channel. The ligand and key amino-acid residues are shown in licorice, the protein is depicted by its inner surface (colored by z-depth). Hydrogen bonds are indicated as yellow dashed lines. The image was generated employing the VMD software (Humphrey et al., 1996). Center: 10.0 ns MD simulation indicating the somewhat labile character of the ligand–protein interactions—particularly of the **47**···Ser61 hydrogen bond. Right: structure of **47**. (For interpretation of the references to colour in this figure legend, the reader is referred to the web version of this article.)

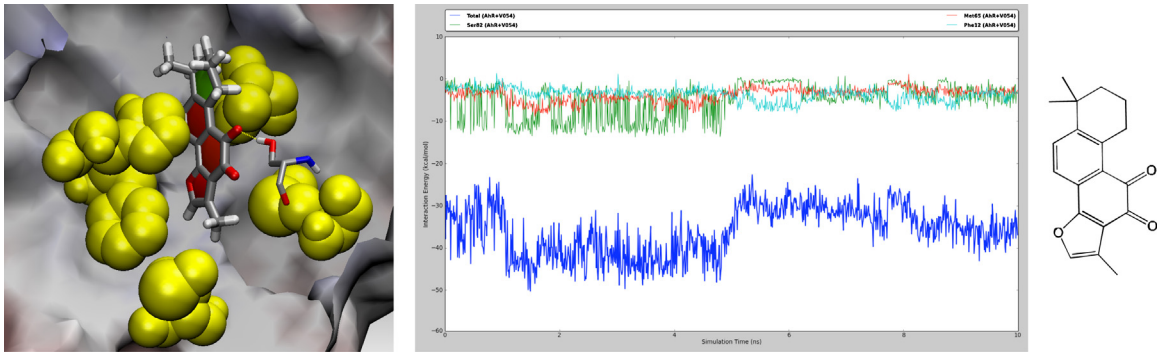

Fig. 7. Left: binding of **54** (tanshinone) to the Aryl hydrocarbon receptor. The ligand and a key amino-acid residue are shown in licorice, hydrophobic residues lining the binding pocket as yellow space-filling spheres, the protein is depicted by its inner surface (colored by z-depth). The hydrogen bond is indicated as a yellow dashed line. The image was generated employing the VMD software (Humphrey et al., 1996). Center: 10.0 ns MD simulation indicating the somewhat labile kinetic character of the ligand–protein interactions. Right: structure of **54**. (For interpretation of the references to colour in this figure legend, the reader is referred to the web version of this article.)

protein, and one carbonyl O atom engages in a hydrogen bond with Ser82 which remains present during 54% of the MD simulation (cf. Table 1). As for hERG, no experimental structure exists for the Aryl hydrocarbon receptor and a homology model is used instead (cf. Vedani, 2016: Table 2). Again, any conclusion drawn therefrom should therefore be interpreted with care. Nonetheless, the quite lipophilic (log P = 2.8—cf. Table 2) and planar compound is reasonably suited to bind to the Aryl hydrocarbon receptor from a structural point of view.

3.4. Metabolic disruption—binding to enzymes of the CYP450 family

Four target proteins in the *VirtualToxLab* belong to the family of the cytochrome P450 enzymes (1A2, 2C9, 2D6, 3A4) and the technology investigates whether a given compound may inhibit these entities, thereby triggering adverse drug–drug interactions. Our simulations indicate that a few compounds can indeed interact with the enzymes and, particularly, bind to the catalytic Fe^{III} ion. Compound **88** binds moderately (0.90 μM) to CYP450 2D6 by

Table 2
Physico-chemical properties of selected compounds employed in this study. Preferred values are given in square brackets. For details, see ref. (Schrödinger, 2011). **M37** is a metabolite of **37** (cf. Fig. 10).

Compound	MW (g/mol)	log P	log S	Oral Abs (%)	Caco Perm (nm/s)	PSA (Å^2)
33	333	0.7	−1.0	74	250	79
37	386	3.6	−4.3	91	240	75
44	460	3.6	−4.4	82	84	113
47	400	4.0	−4.5	93	240	76
54	294	2.8	−3.7	100	1900	57
88	473	4.5	−5.6	100	1200	74
97	299	2.0	−3.8	74	100	104
98	313	2.9	−4.4	91	410	86
M37	402	2.8	−3.8	80	100	94
Eflornithine	182	−2.7	1.0	20	3	95

MW: molecular weight {MW | $130 \leq MW \leq 725$}.
log P: predicted octanol/water partition coefficient {*log* P | $-2.0 \leq log\ P \leq +6.5$}.
log S: predicted aqueous solubility in mol/dm^3 {*log* S | $-6.5 \leq log\ S \leq -0.5$}.
Oral Abs: Predicted human oral absorption on a 0–100% scale {<25% is low, >80% is high}.
Caco Perm: Predicted apparent Caco-2 cell permeability in nm/sec {<25 is poor, >500 is great}.
PSA: polar surface area {PSA | $7 \leq PSA \leq 200$}.

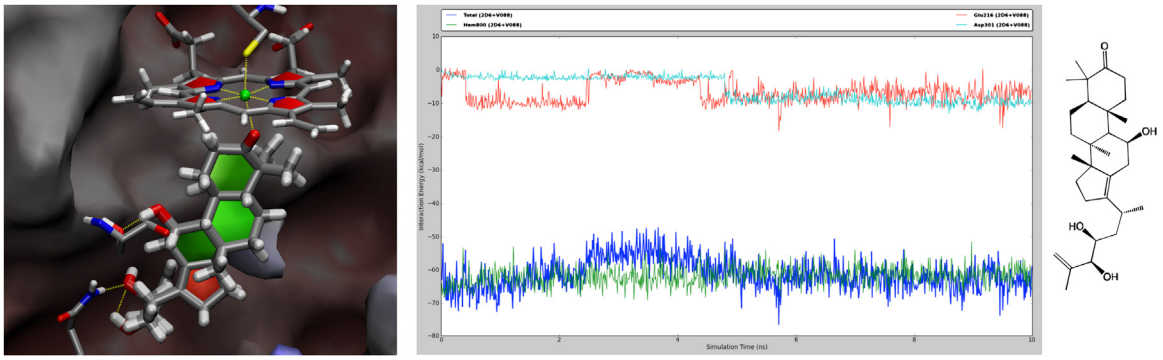

Fig. 8. Left: binding of **88** (as a potential inhibitor) to CYP450 2D6. The ligand, the heme and key amino-acid residues are shown in licorice, the protein is depicted by its inner surface (colored by z-depth); the Fe^{3+} is shown as a green sphere. Hydrogen bonds are indicated as yellow dashed lines. The image was generated employing the VMD software (Humphrey et al., 1996). Center: 10.0 ns MD simulation indicating the quite stable character of the ligand–protein interactions. Right: structure of **88**. (For interpretation of the references to colour in this figure legend, the reader is referred to the web version of this article.)

having its carbonyl O atom coordinated to the metal ion and its hydroxyl groups engaging in hydrogen bonds with Gln244 and Ser304 (Fig. 8: left). The hydrophobic portion of **88** is stabilized by lipophilic residues lining the binding pocket (Phe120, Leu213, Leu241 and Phe483). The 10.0 ns MD simulation indicating the initially labile hydrogen-bond network that becomes stable during the second part of the simulation. The interaction with the heme remains strong throughout the entire simulation. Therefore, the MD simulation (Fig. 8: center) supports the thermodynamic (Monte-Carlo sampling) findings.

Compound **44** binds moderately (1.80 μM) to CYP450 3A4 (Fig. 9). Apart from the interaction of the carbonyl O atom with the heme, a salt bridge of the protonated ammonium moiety with Glu374 contributes strongly to the binding. This interaction remains present throughout the entire simulation. The noticeable gain in the ligand–protein interaction energy after approximately 1.2 ns of simulation time is caused by a slight reorientation of the heme rings (induced fit). However, a binding affinity > 1 μM would not seem to trigger too strong side effects (e.g. drug–drug interactions), except, possibly at long exposure times.

Less problematic than inhibition of an enzyme of the cytochrome P450 series by a compound is its metabolic modification by the enzyme. Nonetheless, it would seem to be appropriate to investigate this mechanism. This was examined by employing version 4.9 of the technology (Vedani et al., 2012), while the most recent version checks for inhibition instead (Vedani et al., 2015) and evaluated the resulting metabolites by the *VirtualToxLab* as well. According to our simulations, **37** would seem to bind to CYP450 2D6 and thereby position a methyl group favorably for a nucleophilic attack (Fig. 10: left). The resulting metabolite—hydroxylated from R-CH_3 to R-CH_2OH (Fig. 10: center and right, highlighted in red) does indeed bind stronger to the glucocorticoid receptor than the parent compound by forming an extra hydrogen bond with Gln642 (Fig. 11). Consequently, the toxic potential of the metabolite is higher (0.632) than that of its parent compound **37** (0.560).

3.5. Derivatives

14 of the investigated sesquiterpene lactones might trigger undesired or unspecific activities due to their *exo*-methylen functionality, which may covalently bind to biological nucleophiles. Therefore, this group has been chemically masked in some compounds (**33R/S**,**36**–**47**). Modifying otherwise too reactive functional groups is a typical strategy in deriving potential drug candidates from natural scaffolds (see, for example, Barnes et al., 2016). According to our calculations, the corresponding natural products display only a low potential (0.178–0.316) to trigger adverse effects. As they were not thought being investigated as potential drug candidates, they are not discussed further here.

3.6. Chemotherapeutic agents—eflornithine

To compare our *in silico* results obtained for the 89 compounds with clinically used antiprotozoal drugs, we have simulated berenil, diminazene, eflornithine, pentamidine and suramin

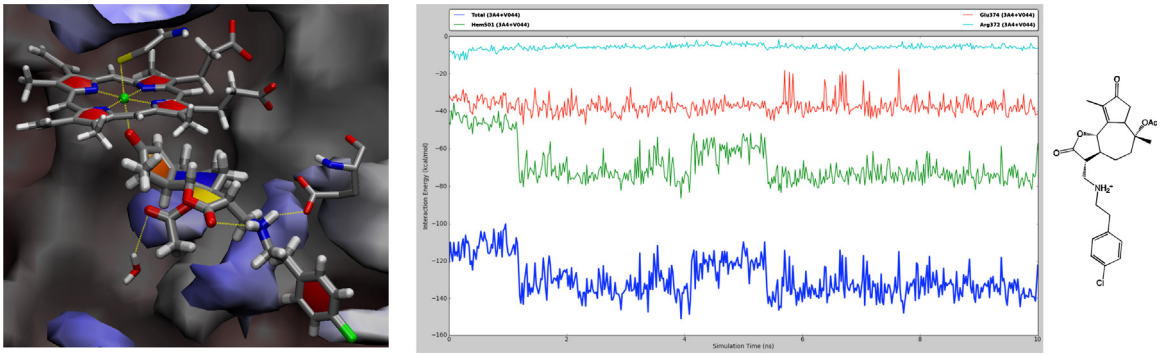

Fig. 9. Left: binding of **44** (as a potential inhibitor) to CYP450 3A4. The ligand, the heme and key amino-acid residues are shown in licorice, the protein is depicted by its inner surface (colored by z-depth); the Fe^{3+} is shown as a green sphere. Hydrogen bonds are indicated as yellow dashed lines. The image was generated employing the VMD software (Humphrey et al., 1996). Center: 10.0 ns MD simulation indicating the overall quite stable character of the ligand–protein interactions. Right: structure of **44**. (For interpretation of the references to colour in this figure legend, the reader is referred to the web version of this article.)

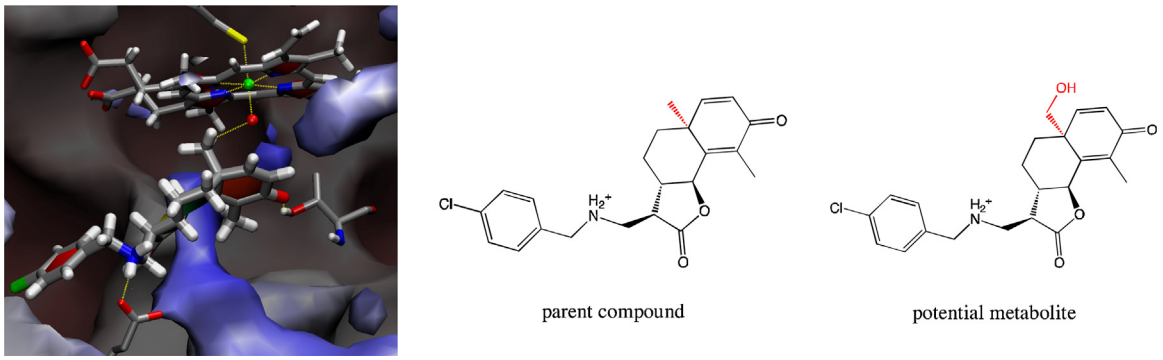

Fig. 10. Interaction of **37** (as a potential substrate) with CYP450 2D6. The heme and **37** are shown in licorice, the iron (green) and the reactive oxygen species (red) as spheres, respectively. The O···H distance of 2.37 Å and the O···H—C angle of 128° suggest an ideal geometry for the nucleophilic attack and the formation of a hydroxylation product. Hydrogen bonds are indicated as yellow dashed lines. The image was generated employing the VMD software (Humphrey et al., 1996). (For interpretation of the references to colour in this figure legend, the reader is referred to the web version of this article.)

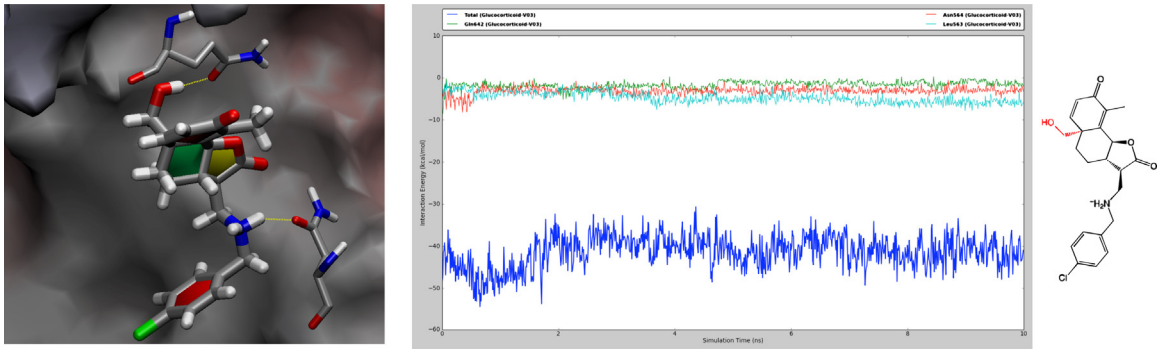

Fig. 11. Left: binding of a potential metabolite of **37** to the glucocorticoid receptor. The ligand and key amino-acid residues are shown in licorice, the protein is depicted by its inner surface (colored by z-depth). Hydrogen bonds are indicated as yellow dashed lines. The image was generated employing the VMD software (Humphrey et al., 1996). Center: 10.0 ns MD simulation indicating the quite stabile character of the ligand–protein interactions. Right: structure of the metabolite. (For interpretation of the references to colour in this figure legend, the reader is referred to the web version of this article.)

employing identical protocols. The most interesting compound with respect to adverse effects (as tested for in the *VirtualToxLab*) is eflornithine, which would seem primarily bind to the Liver-X receptor at a computed affinity of 410 nM but also – albeit at a lower affinities – to the glucocorticoid receptor (1.0 μM), the estrogen receptor α (3.7 μM) and β (2.6 μM), the progesterone receptor (3.6 μM) and the mineralocorticoid receptor (68 μM). This represents a quite interesting bandwidth of potential target proteins might explain some of its side effects, which would seem to be more important than the computed overall toxic potential of moderate 0.412. However, those targets would not seem to be directly associated with the reported side effects triggered by eflornithine (Cook, 1995). Fig. 12 (left) shows the interactions of eflornithine with the Liver-X receptor in detail. The molecule is primarily stabilized by two salt bridges with Arg319 and Glu281, but also through a hydrogen bond with Ser278. The lipophilic part of eflornithine is accommodated by Leu274, Ile277 and Leu330, respectively, lining the lower part of the binding pocket. Fig. 12

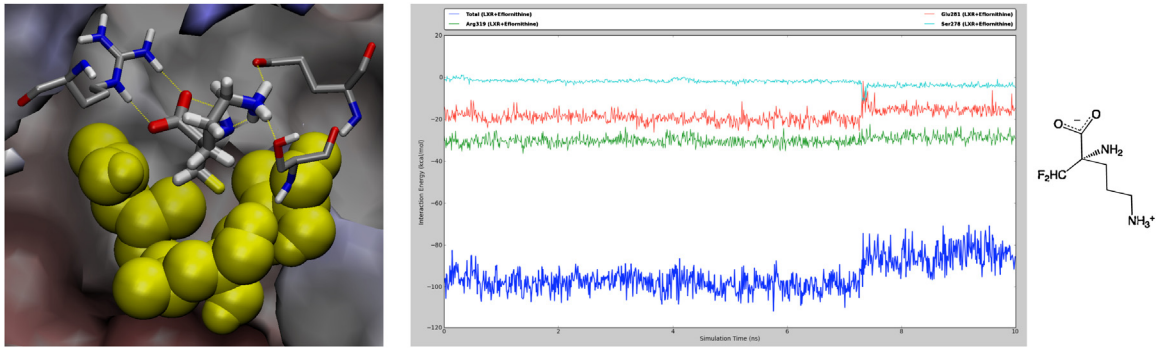

Fig. 12. Left: binding of eflornithine to the Liver-X receptor. The ligand and key amino-acid residues are shown in licorice, hydrophobic residues lining the binding pocket as yellow space-filling spheres, the protein is depicted by its inner surface (colored by z-depth). Hydrogen bonds are indicated as yellow dashed lines. The image was generated employing the VMD software (Humphrey et al., 1996). Center: 10.0 ns MD simulation indicating the quite stabile character of the ligand–protein interactions. Right: structure of eflornithine. Please note that at physiological pH only the terminal amine group is protonated ($pK_{a,calc}$ = 6.9 and 10.1, respectively) while the carboxyl group is certainly deprotonated ($pK_{a,calc}$ = 3.1). (For interpretation of the references to colour in this figure legend, the reader is referred to the web version of this article.)

(center) shows the molecular-dynamical behavior of the compound. While the salt bridge with Arg319 remains stable throughout the entire simulation, the interaction with Glu281 weakens somewhat after approximately 7 ns of simulation time, leading to a moderate overall attenuation of the binding.

3.7. Physico–chemical properties—bioavailability of compounds

Computational assessment of a compound's toxicity should always be discussed along with its ADME properties as those define the bioavailability—a prerequisite for triggering a molecular mechanism leading a toxic effect (Vedani et al., 2015, 2012). To assess the physico–chemical properties of the antitrypanosomal compounds, we employed the *QikProp* software (Schrödinger, 2011) accessible through the *VirtualDesignLab* (Eid et al., 2013). Table 2 shows the key parameters for the compounds discussed in this account. From the point of view of the (computed) solubility, bioavailability, and cell permeability, all compounds would seem to be present at appreciable concentrations in the systemic circulation to trigger the adverse effects discussed above. Interestingly, eflornithrine displays quite opposite values than the natural compounds, i.e. a low lipophilicity and a high solubility combined with a low bioavailability and a poor membrane permeability.

3.8. Consensus scoring—challenging the VirtualToxLab

Although the *VirtualToxLab* employs a sophisticated protocol to assess a compound's toxic potential, both false-positive and false-negative results may occur. False-negative results are more frequent as the technology "only" tests 16 pathways that may eventually manifest a toxic response while many more adverse mechanisms exist (Vedani et al., 2015). Another source for underestimating a compound's harmful character is associated with the fact that exhaustive sampling of ligand binding to a macromolecule is not possible at the currently available computing power, i.e. the correct binding mode might not have been identified, particularly for large and very flexible molecules. The total computing time for the 89 tested compounds amounted to 6189 CPU hours on a Linux cluster (5.2 days of wall-clock time as the longest individual simulation required 125 CPU hours). Exhaustive sampling would imply a 40–80 times longer protocol, which is currently not feasible. Even then, it could not be guaranteed that the correct binding was identified, as induced fit – adaptation of the protein conformation to the ligand's topology – might still not be properly addressed. False-positive results may occur when underestimating a compound's desolvation energy, which, in turn, leads to too high binding affinities or by a structural feasible binding mode that is not retained (stable) throughout a molecular-dynamics simulation.

For an alternative assessment of our compound's harmful character, we have employed three pieces of third-party software: *Toxtree* (Joint Research Centre, 2010a) based on the Cramer rules (Joint Research Centre, 2010b), *MolInspiration* (Molinspiration, 2012a) based on a molecular-fragment database (Molinspiration, 2012b) and *Lazar* (Helma, 2010), using structure–activity relationships (Helma, 2006). The results for the compounds discussed above are given in Table 3.

The *ToxTree* results would seem to be somewhat surprising but they are based on rather simple rules (Joint Research Centre, 2010b), e.g. the occurrence of more than one aromatic ring, the presence of a substituted aromatic ring or any atom other then C, H, O, N or divalent S. If more than two of these conditions are met, a high probability (denoted "++" in Table 3) results. In *MolInspiration*, the most interesting quantity is the probability to bind to a nuclear receptor, which is indeed high for some of the compounds (**54**, **88** and, to a lesser extent, **97**), which is in agreement with our findings. Unfortunately, the binding of **47** to hERG as identified by the *VirtualToxLab* is not conformed by *MolInspiration*, where even a slightly negative probability is calculated. This might be due to the fact, that only heavy but no H atoms are considered in the technology. Protonated N moieties are typical features of hERG blockers—astemizole and cisapride, for example, which are calculated at negative probabilities of −0.06 and 0.15, respectively. Concerning *Lazar*, the six carcinogenicity tests are of particular interest, as the *VirtualToxLab* tests for binding to the aryl hydrocarbon receptor, which is associated with a carcinogenic mechanism. Here, consensus exists on **54**, which is computed to bind at 46 nM to this target. **88**, **89** and **98** also alerted by *Lazar* bind only in the μM range to the aryl hydrocarbon receptor. Again, eflornithrine displays quite different properties than most natural compounds, e.g. a modest probability to bind to ion channels and proteases but much less to nuclear receptors. The latter is in disagreement with the results from our structure-based simulations. However, it is unknown, if and how the zwitter-ionic state of the molecule is taken into consideration by these approaches. In all *VirtualToxLab* and subsequent MD simulations, the protonation state at physiological pH (7.4) was employed (cf. Fig. 12: right).

Table 3
Consensus scoring employing *ToxTree* (Joint Research Centre, 2010a), *MolInspiration* (Molinspiration, 2012a), and Lazar (Helma, 2010). **M37** is a metabolite of **37** (cf. Fig. 10).

Compound	ToxTree	MI/NRL	MI/ICM	MI/PI	MI/EI	Laz/Car	Laz/Mut
33	++	0.37	−0.24	0.01	0.28	0	0
37	++	0.05	−0.16	0.04	0.28	0	0
44	++	0.03	−0.01	0.16	0.29	1	0
47	++	0.01	−0.08	0.13	0.09	0	0
54	++	0.45	−0.06	−0.63	0.22	2	0
88	–	0.81	0.10	0.19	0.64	2	0
97	++	0.12	0.02	0.01	0.08	2	0
98	++	0.05	−0.06	−0.05	0.02	2	0
M37	++	0.12	−0.21	0.08	0.34	0	0
Eflornithine	++	−0.73	0.19	0.14	−0.08	1	0

ToxTree: General harmfulness — low (−), intermediate (+), high (++).
MI/NRL: *MolInspiration*—probability to bind to a nuclear receptor {range | $-1.0 \leq$ range $\leq +1.0$}.
MI/ICM: *MolInspiration*—probability to modulate an ion channel {range | $-1.0 \leq$ range $\leq +1.0$}.
MI/PI: *MolInspiration*—probability to inhibit a protease {range | $-1.0 \leq$ range $\leq +1.0$}.
MI/EI: *MolInspiration*—probability to inhibit an enzyme {range | $-1.0 \leq$ range $\leq +1.0$}.
Laz/Car: *Lazar*—carcinogenicity {six tests: range | $0 \leq$ range ≤ 6}.
Laz/Mut: *Lazar*—mutagenicity {two tests: range | $0 \leq$ range ≤ 2}.

In summary, our studies do not associate a high toxic potential – endocrine and metabolic disruption, as well as aspects of carcinogenicity and cardiotoxicity – to the investigated 89 natural compounds and derivatives with antitrypanosomal activity and neither do (with exception of *ToxTree*) the other employed software tools. Of course, adverse effects might be triggered via a wealth of mechanisms, only a few of which have been simulated in this study. As natural products, in contrast to classic synthetic drugs, often feature a complex topology decorated with a larger number of hydrogen-bond functionalities, it is less likely that they meet another (off-) targets binding pattern than rather simple chemotherapeutic compounds, e.g. the antitrypanosomal small-molecule drug diminazene. On the other hand, the unique configuration of natural compounds might privilege them to trigger more complex agonistic mechanisms.

4. Conclusions

To investigate potential side effects triggered by antitrypanosomal natural products and derivatives, we combined the

VirtualToxLab (simulation and quantification of small-molecule binding to nuclear receptors, enzymes of the CYP450 family, the Aryl hydrocarbon receptor and the hERG ion channel) and molecular-dynamics simulations in consensus mode (three different pieces of software). While the former addresses "thermodynamic" binding, the latter probe the kinetic stability of ligand–protein complexes. Among the 89 tested compounds, we identified a paprazine derivative to bind strongly and kinetically stable to the androgen receptor, thereby possibly leading to endocrine disruption. One other compound each would seem to interact with the aryl hydrocarbon receptor and hERG, respectively. With one exception, the investigated metabolites are not expected to trigger stronger effects than their parent compounds. Finally, we compared our results with those obtained by third-party software aimed at estimating adverse effects. In summary, the investigated compounds would not seem to represent an immediate health risk but a few of them might, at longer exposure, trigger undesirable effects. From computational studies, highly decorated complex molecular topologies of natural compounds would seem to be less prone to trigger adverse effects than simpler chemical structures (as employed in classic therapies) which may easier bind to undesired off-targets (see, for example Biographics Laboratory 3R, 2016b: results on 2666 tested compounds as well as Ekins, 2014; Roberts, 2010).

Conflict of interest

The authors declare no conflict of interest.

Acknowledgement

Financial support by the *Swiss National Foundation* (grant SNF 205321_135678) for this work is gratefully acknowledged.

Appendix A. Supplementary data

Supplementary data associated with this article can be found, in the online version, at http://dx.doi.org/10.1016/j.toxlet.2016.04.013.

Compound structures and SMILES codes, binding affinities, details on the molecular-dynamics simulations

References

Amini, A., Mugleton, S.H., Lohdi, H., Sternberg, M.J.E., 2007. A novel logic-based approach for quantitative toxicology prediction. J. Chem. Inf. Model. 47, 998–1006.

Aronov, A.M., Balakin, K.V., Kiselyov, A., Varma-O'Brien, S., Ekins, S., 2007. Application of QSAR to ion channels. In: Ekins, S. (Ed.), Computational Toxicology—Risk Assessment for Pharmaceutical and Environmental Chemicals. J. Wiley & Sons, New York, NY, USA, pp. 353–390.

Ayyari, M., Salehi, P., Ebrahimi, S.N., Zimmermann, S., Portmann, L., Krauth-Siegel, R. L., Kaiser, M., Brun, R., Rezadoost, H., Rezazadeh, S., Hamburger, M., 2014. Antitrypanosomal isothiocyanate and thiocarbamate glycosides from *Moringa peregrine*. Planta Med. 80, 86–89.

Banks, J.L., Beard, H.S., Cao, Y., Cho, A.E., Damm, W., Farid, R., Felts, A.K., Halgren, T.A., Mainz, D.T., Maple, J.R., Murphy, R., Philipp, D.M., Repasky, M.P., Zhang, L.Y., Berne, B.J., Friesner, R.A., Gallicchio, E., Levy, R.M., 2005. Integrated modeling program, applied chemical theory (IMPACT). J. Comp. Chem. 26, 1752–1780.

Barnes, E.C., Kumar, R., Davis, R.A., 2016. The use of isolated natural products as scaffolds for the generation of chemically diverse screening libraries for drug discovery. Nat. Prod. Rep. doi:http://dx.doi.org/10.1039/C5NP00121H (advance article).

Bars, R., Broeckaert, F., Fegert, I., Gross, M., Hallmark, N., Kedwards, T., Lewis, D., O'Hagan, S., Panter, G.H., Weltje, L., Weyers, A., Wheeler, J.R., Galay-Burgos, M., 2011. Science based guidance for the assessment of endocrine-disrupting properties of chemicals. Regul. Toxicol. Pharmacol. 59, 37–46.

Bender, A., Scheiber, J., Glick, M., Davies, J.W., Azzaoui, K., Hamon, J., Urban, L., Whitebread, S., Jenkins, J.L., 2007. Analysis of pharmacology data and the prediction of adverse drug reactions and off-target effects from chemical structure. ChemMedChem 2, 861–873.

Benfenati, E. (Ed.), 2016. In Silico Methods for Predicting Drug Toxicity. Springer, Berlin/New York, pp. 632 Available at http://dx.doi.org/10.1007/978-1-4939-3609-0 (accessed 08.04.16.).

Benfenati, E., Begigni, R., DeMarini, D.M., Helma, C., Kirkland, D., Martin, T.M., Mazzatorta, P., Quédraogo-Arras, G., Richard, A.M., Schilter, B., Schoonen, W.G.E. J., Snyder, R.D., Yang, C., 2009. Predictive models for carcinogenicity and mutagenicity: frameworks state-of-the-art, and perspectives. J. Environ. Sci. Health Part C 27, 57–90.

Best, R.B., Zhu, X., Shim, J., Lopes, P.E.M., Mittal, J., Feig, M., MacKerell, A.D., 2012. Optimization of the additive CHARMM all-atom protein force field. J. Chem. Theory Comput. 8, 3257–3273.

Biographics Laboratory 3R, 2016a. Available at http://www.biograf.ch/data/home/Validation_5.8. Y.3_dble.png (accessed 08.04.16.).

Biographics Laboratory 3R, 2016b. Available at http://www.biograf.ch/data/projects/virtualtoxlab_results.php (accessed 08.04.16.).

Case, D.A., Darden, T.A., Cheatham III, T.A., Simmerling, C.L., Wang, J., Duke, R.E., Luo, R., Walker, R.C., Zhang, W., Merz, K.M., Roberts, B., Hayik, S., Roitberg, A., Seabra, G., Swails, J., Götz, A.W., Kolossváry, I., Wong, K.F., Paesani, F., Vanicek, J., Wolf, R. M., Liu, J., Wu, X., Brozell, S.R., Steinbrecher, T., Gohlke, H., Cai, Q., Ye, X., Wang, J., Hsieh, M.J., Cui, C., Roe, D.R., Mathews, D.H., Seetin, M.G., Salomon-Ferrer, R., Sagui, C., Babin, V., Luchko, T., Gusarov, S., Kovalenko, A., Kollman, P.A., 2012. AMBER 12. University of California, San Francisco.

Case, D.A., Babin, V., Berryman, J.T., Betz, R.M., Cai, Q., Cerutti, D.S., Cheatham III, T.A., Darden, T.A., Duke, R.E., Gohlke, H., Gietz, A.W., Gusarov, S., Homeyer, N., Jonowski, P., Kaus, J., Kolossváry, I., Kovalenko, A., Lee, T.S., LeGrand, S., Luchko, T., Luo, R., Madei, B., Merz, K.M., Paesani, F., Roe, D.R., Roitberg, A., Sagui, C., Salomon-Ferrer, R., Seabra, G., Simmerling, C.L., Smith, W., Swails, J., Walker, R. C., Wang, J., Wolf, R.M., Wu, X., Kollman, P.A., 2014. AMBER 14. University of California, San Francisco.

Cook, C.G., 1995. Adverse effects of chemotherapeutic agents used in tropical medicine. Drug Saf. 13, 31–45.

Cronin, M.T.D., Madden, J.C., 2010. In Silico Toxicology. RSC Publishing, Cambridge, UK.

Custer, L.L., Kreatsoulas, C., Durham, S.K., 2007. Predicitve mutagenicity computer models. In: Ekins, S. (Ed.), Computational Toxicology—Risk Assessment for Pharmaceutical and Environmental Chemicals. J. Wiley & Sons, New York, NY, USA, pp. 391–401.

Darden, T., York, D., Pedersen, L., 1993. J. Chem. Phys. 98, 10089–10092.

De Olivera, S.K., Domeneghini Chiaradia-Delatorre, L., Mascarello, A., Veleirunho, B., Ramlov, F., Kuhnen, S., Yunes, A., Maraschin, M., 2015. From bench to bedside: natural products and analogs for the treatment of neglected tropical diseases. In: Rahman, A. (Ed.), Studies in Natural Products Chemistry, vol. 44. Elsevier, Amsterdam, pp. 33–92.

Dobler M., 2014. Bio^{X}—a versatile molecular-modeling software. Biographics Laboratory 3R, Basel. Freely available at http://www.biograf.ch/index.php?id=software (accessed 08.04.16.).

Ecker, G.F., Chiba, P., 2007. QSAR studies on drug transporters involved in toxicology. In: Ekins, S. (Ed.), Computational Toxicology—Risk Assessment for Pharmaceutical and Environmental Chemicals. J. Wiley & Sons, New York, NY, USA, pp. 295–314.

Eid, S., Zalewski, A., Smieško, M., Ernst, B., Vedani, A., 2013. A molecular-modeling toolbox aimed at bridging the gap between medicinal chemistry and computational sciences. Int. J. Mol. Sci. 14, 684–700.

Ekins, S., 2007. Application of QSAR to enzymes involved in toxicology. In: Ekins, S. (Ed.), Computational Toxicology—Risk Assessment for Pharmaceutical and Environmental Chemicals. J. Wiley & Sons, New York, NY, USA, pp. 277–294.

Ekins, S., 2014. Progress in computational toxicology. J. Pharmacol. Toxicol. Methods 69, 115–140.

Enoch, S.J., Cronin, M.T.D., Schultz, T.W., Madden, J.C., 2008. Quantitative and mechanistic read across for predicting the skin sensitization potential of alkenes acting via Michael addition. Chem. Res. Toxicol. 21, 513–520.

Farimani, M.M., Bahadori, M., Taheri, B.S., Ebrahimi, N.S., Zimmermann, S., Brun, R., Amin, G., Hamburger, M., 2011. Triterpenoids with rare carbon skeletons from *Salvia hydrangea*: antiprotozoal activity and absolute configurations. J. Nat. Prod. 74, 2200–2205.

Green, N., Naven, R., 2009. Early toxicity screening strategies. Curr. Opin. Drug Discov. Dev. 12, 90–97.

Gupta, S., Kapoor, P., Chaudhari, K., Gautam, A., Kumar, R., Raghava, G.P.S., 2013. In silico approach for predicting toxicity of peptides and proteins. PLoS One 8 e73957, 29.

Hata, Y., Zimmermann, S., Quitschau, M., Kaiser, M., Hamburger, M., Adams, M., 2011. Antiplasmodial and antitrypanosomal activity of pyrethrins and pyrethroids. J. Agric. Food Chem. 59, 9172–9176.

Helma, C., 2006. Lazy structure–activity relationships (Lazar) for the prediction of rodent carcinogenicity and *Salmonella* mutagenicity. Mol. Divers. 10, 147–158.

Helma, C., 2010. Available at http://lazar.in-silico.ch/predict (accessed 08.04.16.).

Hotez, P.J., Molyneuz, D.H., Fenwick, A., Kumaresan, J., Sachs, S.E., Sachs, J.D., Savioloi, L., 2007. Control of neglected tropical diseases. N. Engl. J. Med. 357, 1018–1027.

Hu, Z., 2015. Docking, scoring and binding-affinity prediction in computer-aided drug discovery. Dissertation. University of Basel, Switzerland.

Humphrey, W., Dalke, A., Schulten, K., 1996. VMD—visual molecular dynamics. J. Mol. Graph. 14, 33–38.

Joint Research Centre, 2010a. Available at http://toxtree.sourceforge.net (accessed 08.04.16.).

Joint Research Centre, 2010b. Available at https://eurl-ecvam.jrc.ec.europa.eu/laboratories-research/predictivetoxicology/doc/Toxtree_Cramer_extensions.pdf (accessed 08.04.16.).
Julian, T., Hata, Y., Zimmermann, S., Kaiser, M., Hamburger, M., Adams, M., 2011. Antitrypanosomal sesquiterpene lactones from *Saussurea costus*. Fitoterapia 82, 955–959.
Kavlock, R.J., Ankley, G., Blancato, J., Breen, M., Conolly, R., Dix, D., Houck, K., Hubal, E., Judson, R., Rabinovitz, J., Richard, A., Setzer, R.W., Shah, I., Villeneuve, D., Weber, E., 2008. Computational toxicology—a state of the science mini review. Toxicol. Sci. 103, 14–27.
Kellenberger, E., Hofmann, A., Quinn, R.J., 2011. Similar interactions of natural products with biosynthetic enzymes and therapeutic targets could explain why nature produces such a large proportion of existing drugs. Nat. Prod. Rep. 28, 1483–1492.
Kerrigan, J.E., 2013. Molecular dynamics simulations in drug design. In: Clifton, N.J. (Ed.), Methods in Molecular Biology, vol. 993. Springer, Berlin/New York, pp. 95–113.
Merlot, C., 2008. In silico methods for early toxicity assessment. Curr. Opin. Drug Discov. Dev. 11, 80–85.
Mohamadi, F., Richards, N.G.J., Guida, W.C., Liskamp, R., Lipton, M., Caufield, C., Chang, G., Hendrickson, T., Still, W.C., 1990. MacroModel—an integrated software system for modeling organic and bioorganic molecules using molecular mechanics. J. Comp. Chem. 11, 440–467.
Molinspiration, 2012a. Available at http://www.molinspiration.com/cgi-bin/properties (accessed 08.04.16.).
Molinspiration, 2012b. Available at http://www.molinspiration.com/docu/miscreen/druglikeness.html (accessed 08.04.16.).
Mortier, J., Rakers, C., Bermudes, M., Murgeito, M.S., Riniker, S., Wolber, G., 2015. The impact of molecular dynamics on drug design: applications for the characterization of ligand–macromolecule complexes. Drug Discov. Today 20, 686–702.
Nigsch, F., Macaluso, N.J.M., Mitchell, J.B.O., Zmuidinavicus, D., 2009. Computational toxicology: an overview of the sources of data and modeling methods. Exp. Opin. Drug Metab. Toxicol. 5, 1–14.
Orhan, I., Sener, B., Kaiser, M., Brun, R., Tasdemir, D., 2010. Inhibitory activity of marine sponge-derived natural products. Mar. Drugs 8, 47–58.
Pavan, M., Worth, A., 2008. Publicly accessible QSAR software tools developed by the Joint Research Centre. SAR QSAR Environ. Res. 19, 785–799.
Phillips, C., Braun, R., Wang, W., Gumbart, J., Tajkhorshid, E., Villa, E., Chipot, C., Skeel, R., Kale, R., Schulten, K., 2005. Scalable molecular dynamics with NAMD. J. Comp. Chem. 26, 1781–1802.
Piclin, N., Pintore, M., Wechman, C., Roncaglioni, A., Benfenati, E., Chretien, J.R., 2006. Ecotoxicity prediction by adaptive fuzzy-partitioning: comparing descriptors computed on 2D and 3D structures. SAR QSAR Environ. Res. 17, 225–251.
Roberts, D.W., 2010. Mechanisms of toxic action in *in silico* toxicology. In: Cronin, M. T.D., Madden, J.C. (Eds.), In Silico Toxicology—Principles and Applications. RSC Publishing, Cambridge, pp. 334–345.
Roncaglioni, A., Toropov, A.A., Toropova, A.P., Benfenati, E., 2013. In silico methods to predict drug toxicity. Curr. Opin. Pharmacol. 13, 802–806.
Rossato, G., Ernst, B., Smieško, M., Spreafico, M., Vedani, A., 2010. Probing small-molecule binding to cytochrome P450 2D6 and 2C9: an in silico protocol for generating toxicity alerts. ChemMedChem 5, 2088–2101.
S'lusarczyk, S., Zimmermann, S., Kaiser, M., Matkowski, A., Hamburger, M., Adams, M., 2011. Antiplasmodial and antitrypanosomal activity of tanshinone-type diterpenoids from *Salvia miltiorrhiza*. Planta Med. 77, 1594–1596.
Schilter, B., Benigni, R., Boobis, A., Chiodini, A., Cockburn, A., Cronin, M.T.D., Lo Piparo, E., Modi, S., Thiel, A., Worth, A., 2014. Establishing the leval of safety concern for chemicals in food without the need for toxicity testing. Regul. Toxicol. Pharmacol. 68, 275–296.
Schrödinger, LLC, 2011. QikProp, version 3.4. New York, NY, USA
Serafimova, R., Todorov, M., Pavlov, T., Kotov, S., Jacob, E., Aptula, A., Mekenyan, O., 2007. Identification of the structural requirements of mutagenicity by incorporating molecular flexibility and metabolic activation of chemicals. II. General Ames mutagenicity model. Chem. Res. Toxicol. 20, 662–676.
Shah, F., Greene, N., 2014. Analysis of Pfizer compounds in EPA's ToxCast chemical-assay space. Chem. Res. Toxicol. 27, 86–98.
Singh, K.P., Gupta, S., 2014. In silico prediction of toxicity of non-congeneric industrial chemicals using ensemble-learning based modeling approaches. Toxicol. Appl. Pharmacol. 275, 198–212.
Smieško, M., 2013. Dolina—docking based on a local induced-fit algorithm: application toward small-molecule binding to nuclear receptors. J. Chem. Inf. Model. 53, 1415–1423.
Spreafico, M., Smieško, M., Lill, M.A., Ernst, B., Vedani, A., 2009. Mixed-model QSAR at the glucocorticoid receptor: predicting the binding mode and affinity of psychotropic drugs. ChemMedChem 4, 100–109.
Toropov, A.A., Toropova, A.P., Raska Jr., I., Leszcynska, D., Leszcynski, J., 2014. Comprehension of drug toxicity: software and databases. Comp. Biol. Med. 45, 20–25.
Usuki, T., Sato, M., Hara, S., Yoshimoto, Y., Kondo, R., Zimmermann, S., Kaiser, M., Brun, R., Hamburger, M., Adams, M., 2014. Antitrypanosomal structure-activity relationship study of synthetic cynaropicrin derivatives. Bioorg. Med. Chem. Lett. 24, 794–798.
Valerio Jr., L.G., 2009. In silico toxicology for the pharmaceutical sciences. Toxicol. Appl. Pharmacol. 241, 356–370.
Vedani, A., 2016. VirtualToxLab user manual. Available at www.biograf.ch/downloads/VirtualToxLab.pdf (accessed 08.04.16.).
Vedani, A., Huhta, D.W., 1990. A new force field for modeling metalloproteins. J. Am. Chem. Soc. 112, 4759–4767.
Vedani, A., Dobler, M., Smieško, M., 2012. VirtualToxLab—a platform for estimating the toxic potential of drugs, chemicals and natural products. Toxicol. Appl. Pharmacol. 261, 142–153.
Vedani, A., Dobler, M., Hu, Z., Smieško, M., 2015. OpenVirtualToxLab—a platform for generating and exchanging in silico toxicity data. Tox. Lett. 232, 519–532 Available at http://dx.doi.org/10.1016/j.toxlet.2014.09.004 (accessed 08.04.16.).
Vuorinen, A., Odermatt, A., Schuster, D., 2013. In silico methods in the discovery of endocrine-disrupting chemicals. J. Steroid Biochem. Mol. Biol. 137, 18–26.
Worth, A.P., Cronin, M.T.D., 2004. Report of the workshop on the validation of QSARs and other computational prediction models. ATLA 32 (Suppl. 1), 703–706.
Zhao, H., Cafliesch, A., 2015. Molecular dynamics in drug design. Eur. J. Med. Chem. 91, 4–14.
Zimmermann, S., Fouché, M., DeMieri, Yoshimoto, Y., Usuki, T., Nthambeleni, R., Parkinson, C.J., Westhuyzen, C.V., Kaiser, M., Hamburger, M., Adams, M., 2014. Structure–activity relationship study of sesquiterpene lactones and their semi-synthetic amino derivatives as potential antitrypanosomal products. Molecules 19, 3523–3538.